

Informatics Tools for Tumor Heterogeneity in Multiplexed Fluorescence Images

*chakra chennubhotla** and
brion sarachan⁺

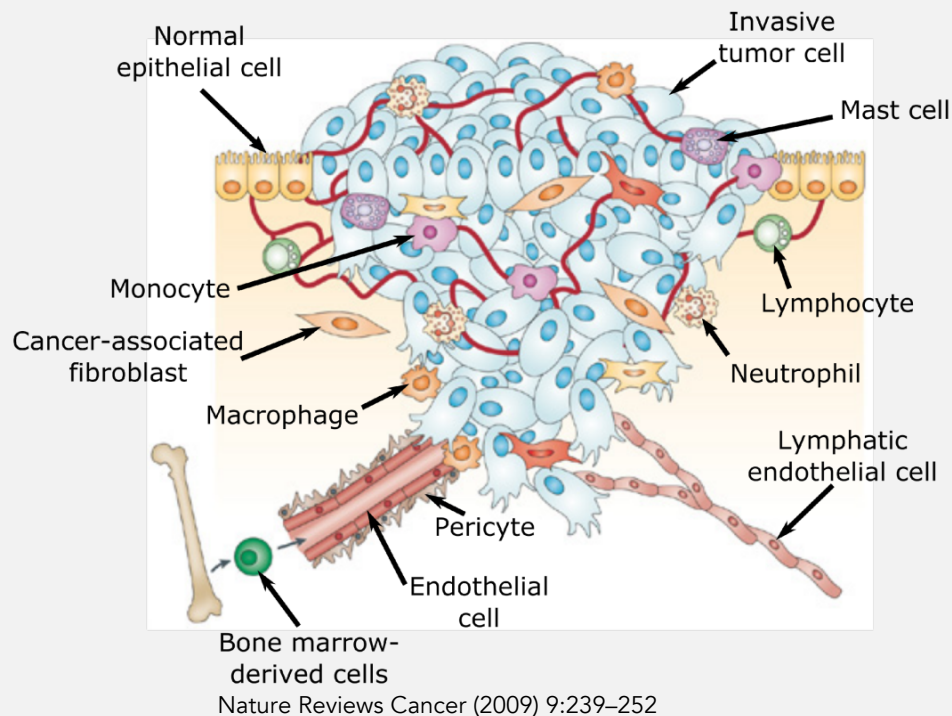
**university of pittsburgh*

⁺GE global research center

Research reported in this publication was supported by the National Cancer Institute of the National Institute of Health under award number U01CA204826. The content is solely the responsibility of the authors and does not necessarily represent the official views of the National Institute of Health.

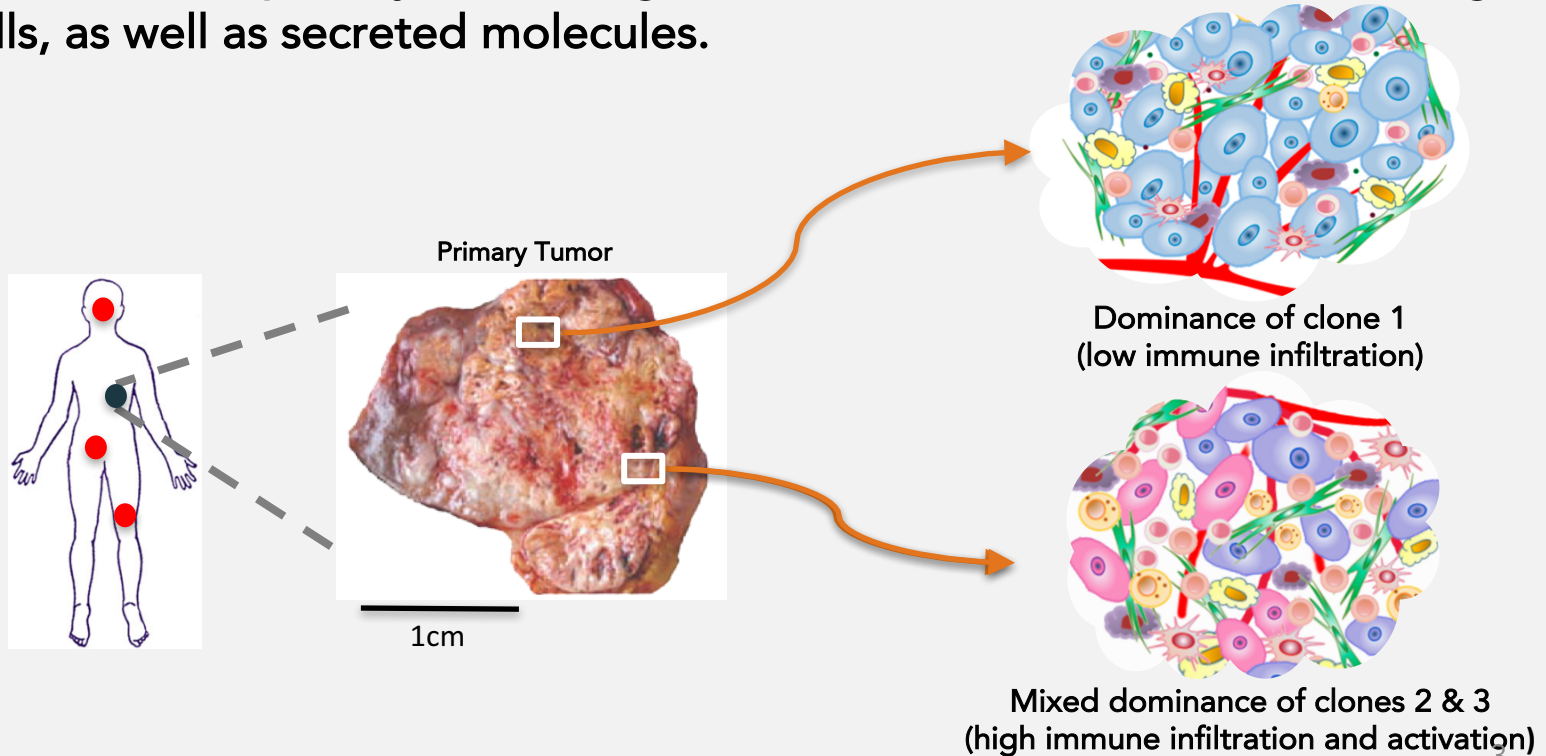
Tumor heterogeneity and cell-cell communication in TME play a critical role in drug resistance and metastasis.

Critical knowledge gap in how different cell types in a TME simultaneously collaborate to drive invasion/metastasis and therapeutic resistance phenotypes.



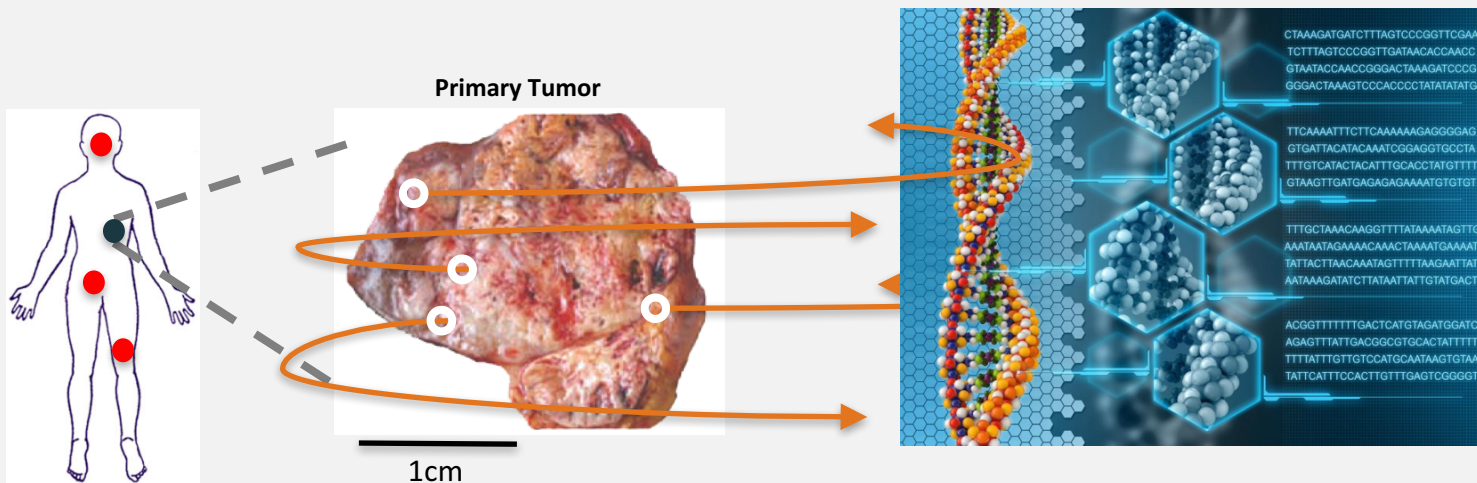
Quantifying spatial intratumor heterogeneity is critical for accurate diagnosis and prognosis

Primary tumors represent evolving eco-systems comprised of distinct microenvironments of spatially interacting cancer and non-cancer cells, including immune cells, as well as secreted molecules.



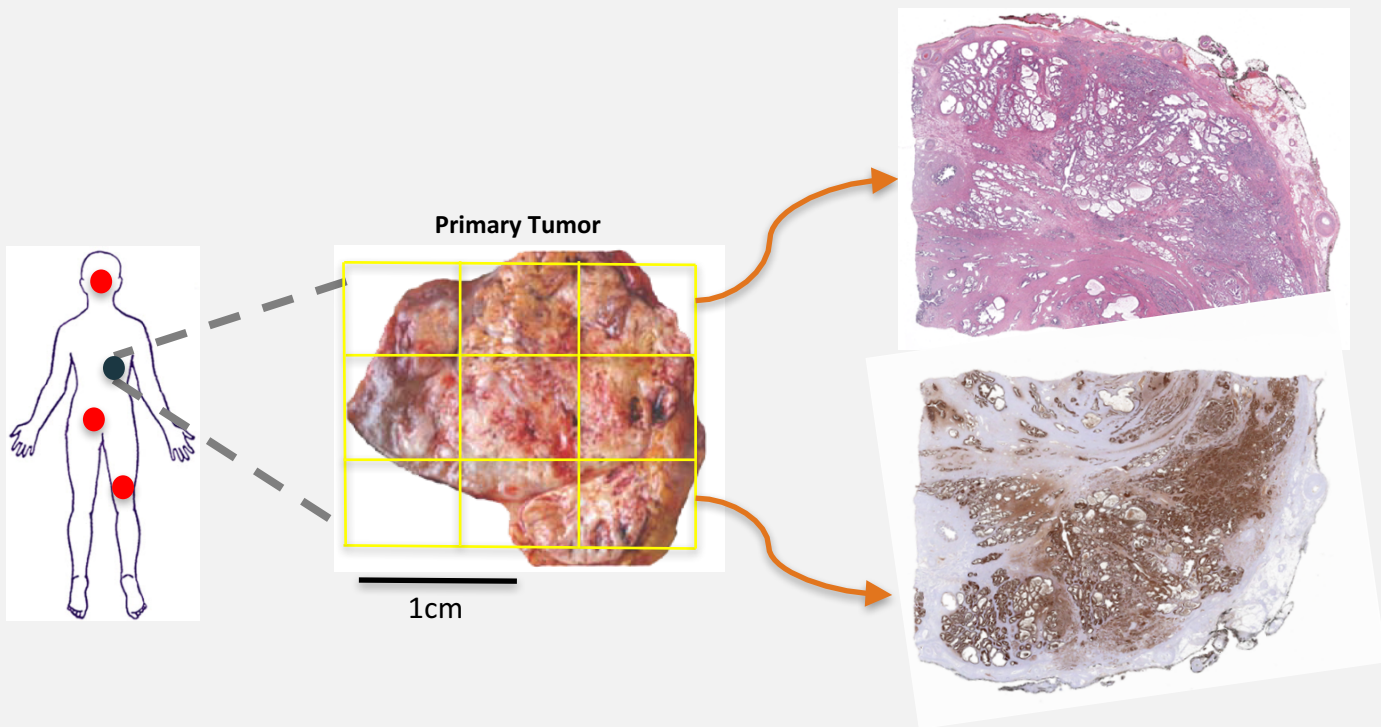
Today's Clinical Practice Fails to Predict Tumor Progression

Current genomic analyses alone do not directly capture the critical spatial interactions in tumors responsible for metastasis.



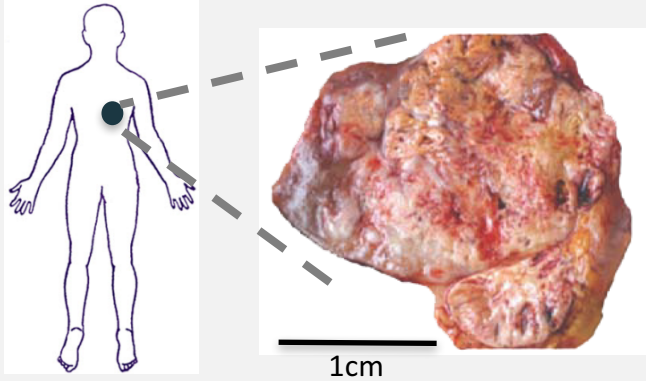
Today's Clinical Practice Fails to Predict Tumor Progression

In addition, the current practice of pathology yields insufficient molecular details of spatial interactions within tumor microenvironments.



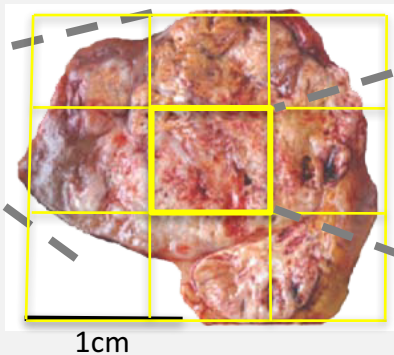
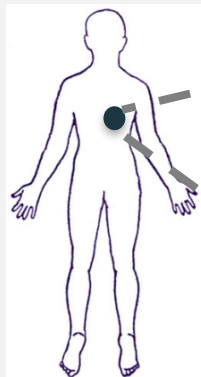
Computational Spatial Tumor Pathology

The measurement of multiple biomarkers in tissue sections coupled with machine learning tools characterizes the spatial interactions and infers signaling networks responsible for tumor progression.

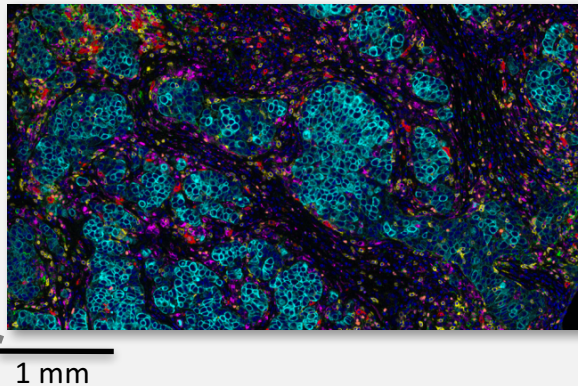


Computational Spatial Tumor Pathology

The measurement of multiple biomarkers in tissue sections coupled with machine learning tools characterizes the spatial interactions and infers signaling networks responsible for tumor progression.

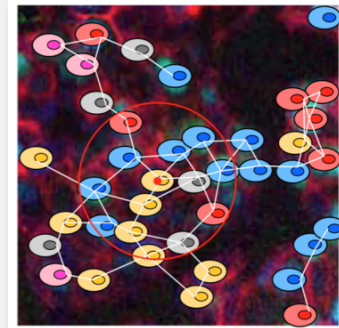
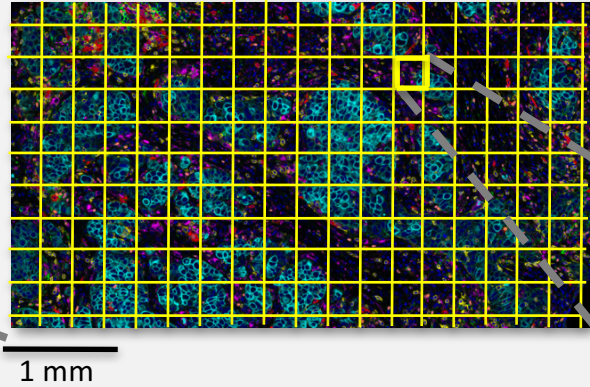
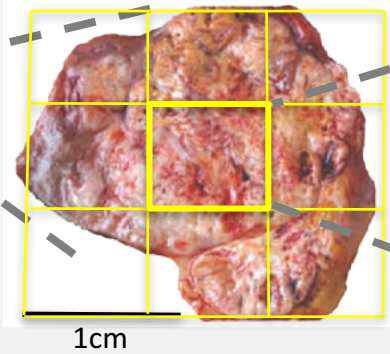
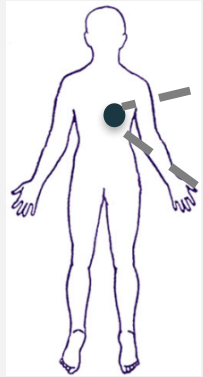


Multi to hyperplexed IF



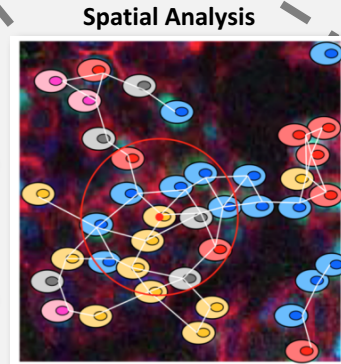
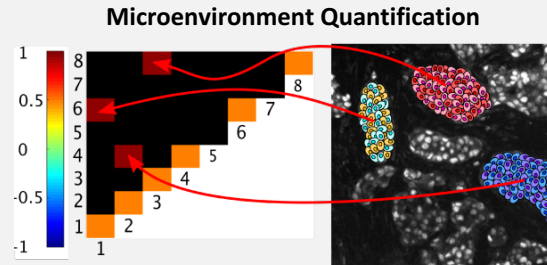
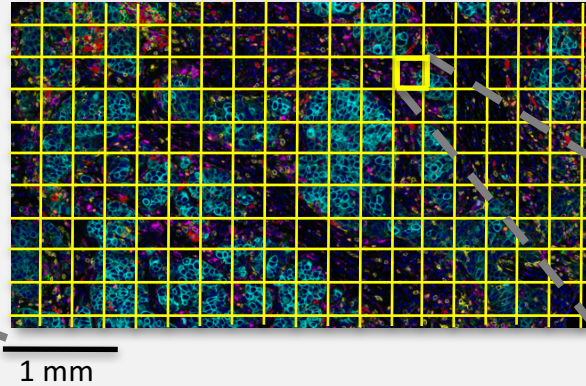
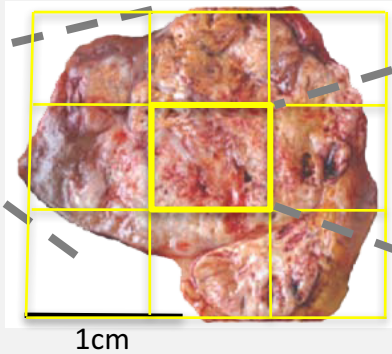
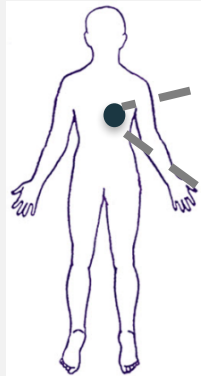
Computational Spatial Tumor Pathology

The measurement of multiple biomarkers in tissue sections coupled with machine learning tools characterizes the spatial interactions and infers signaling networks responsible for tumor progression.



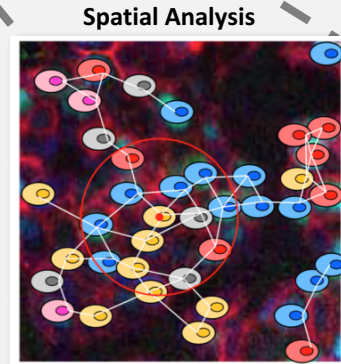
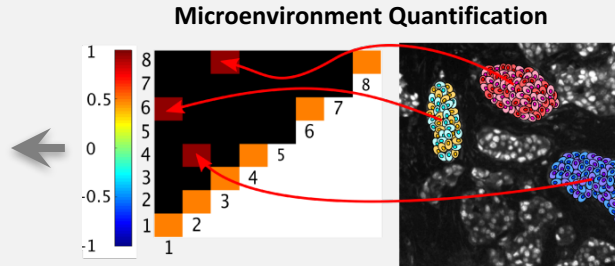
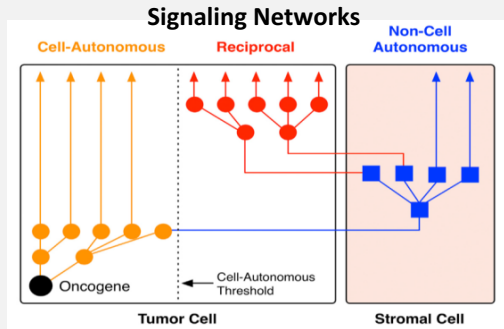
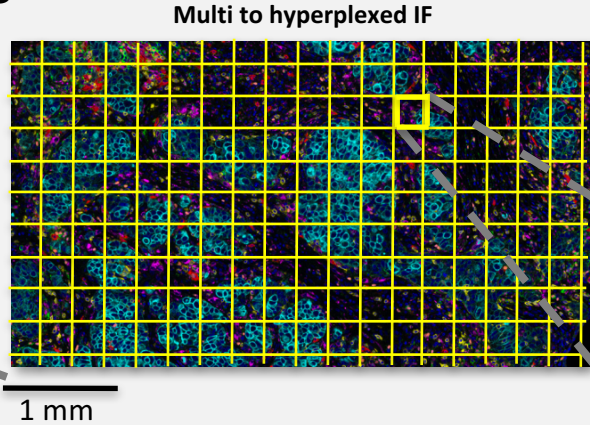
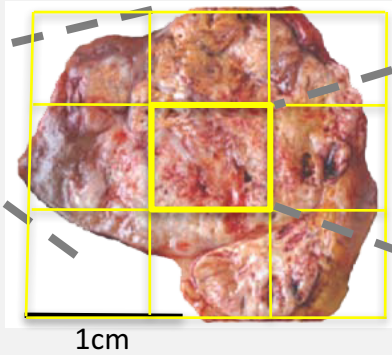
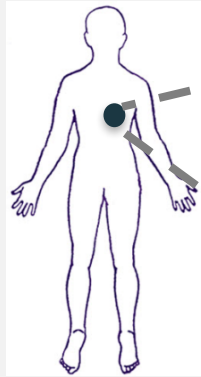
Computational Spatial Tumor Pathology

The measurement of multiple biomarkers in tissue sections coupled with machine learning tools characterizes the spatial interactions and infers signaling networks responsible for tumor progression.



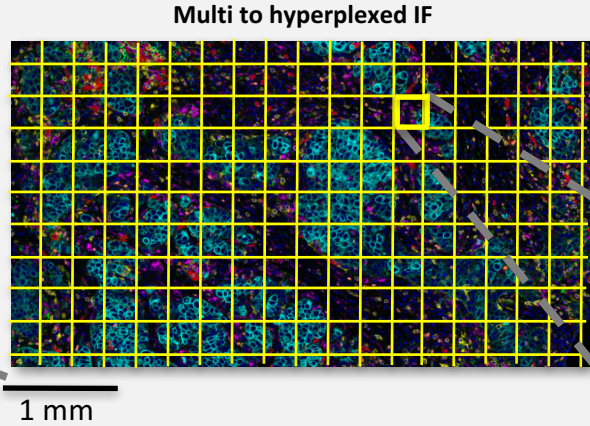
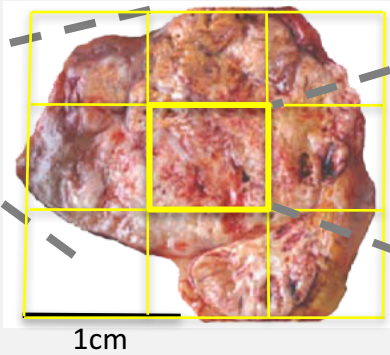
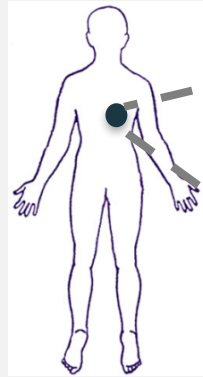
Computational Spatial Tumor Pathology

The measurement of multiple biomarkers in tissue sections coupled with machine learning tools characterizes the spatial interactions and infers signaling networks responsible for tumor progression.



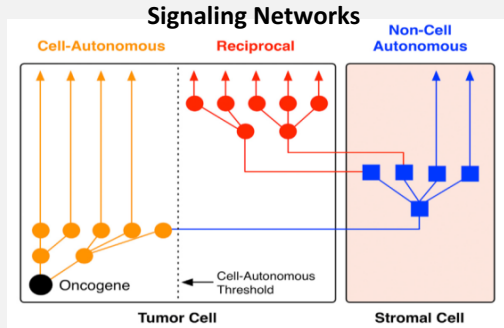
Computational Spatial Tumor Pathology

Characterizing the critical spatial interactions of tumor microenvironments leads to improved diagnoses, prognoses, and therapeutic strategies.

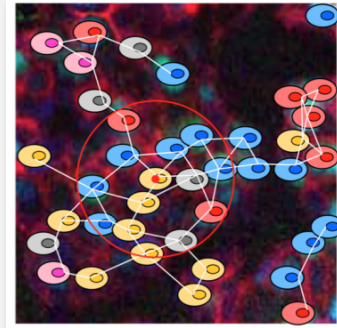
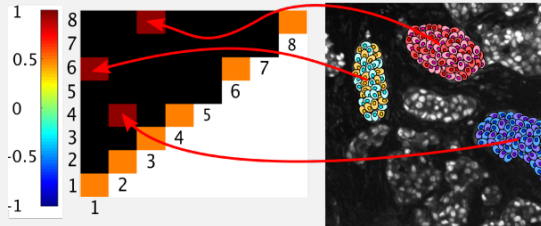


Spatial Analysis

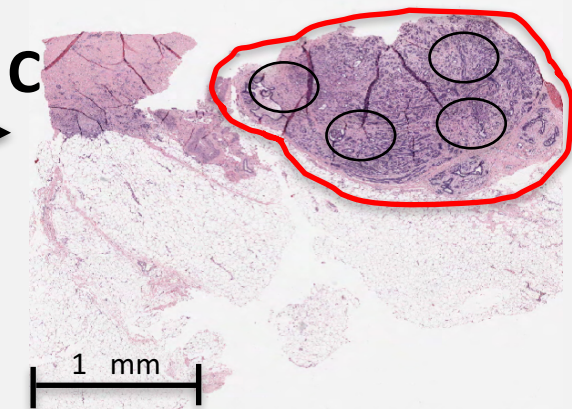
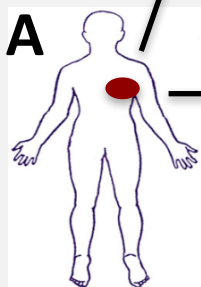
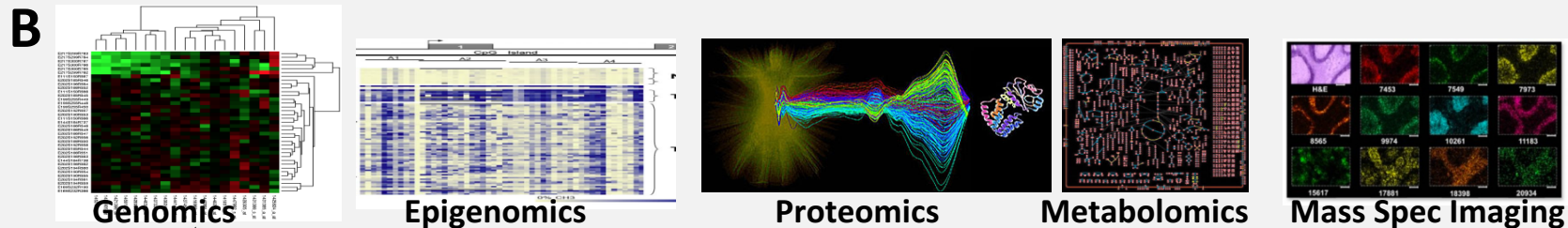
Diagnosis, Prognosis & Therapeutic Strategy



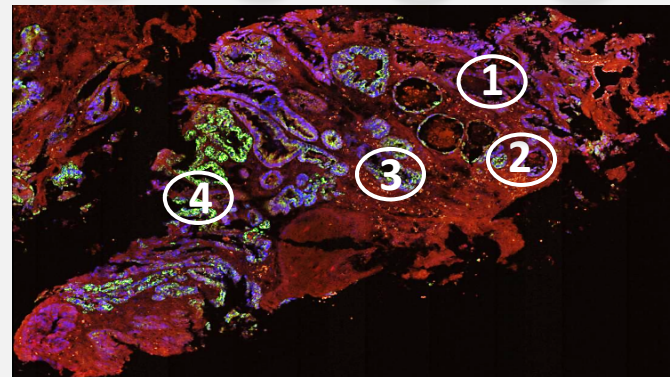
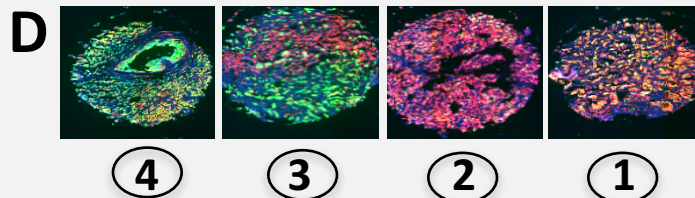
Microenvironment Quantification



Computational Spatial Tumor Pathology



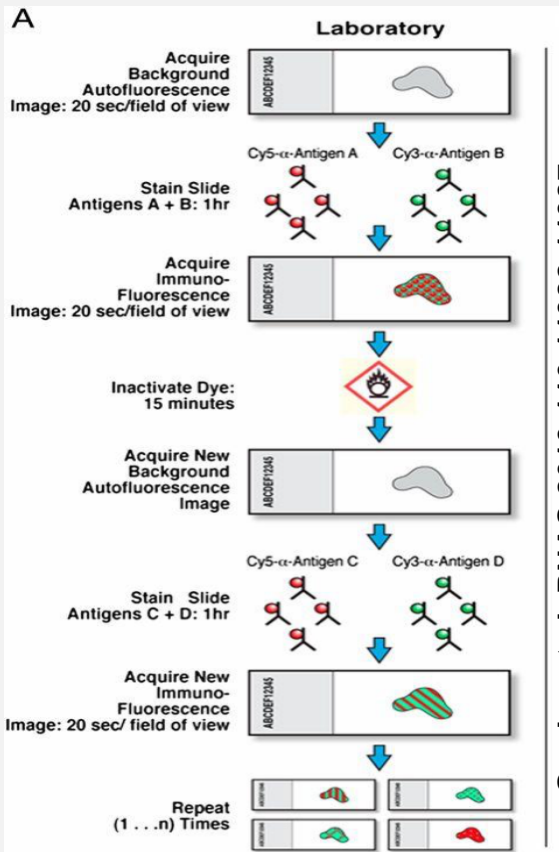
H&E stained whole tissue section from FFPE tumor sample



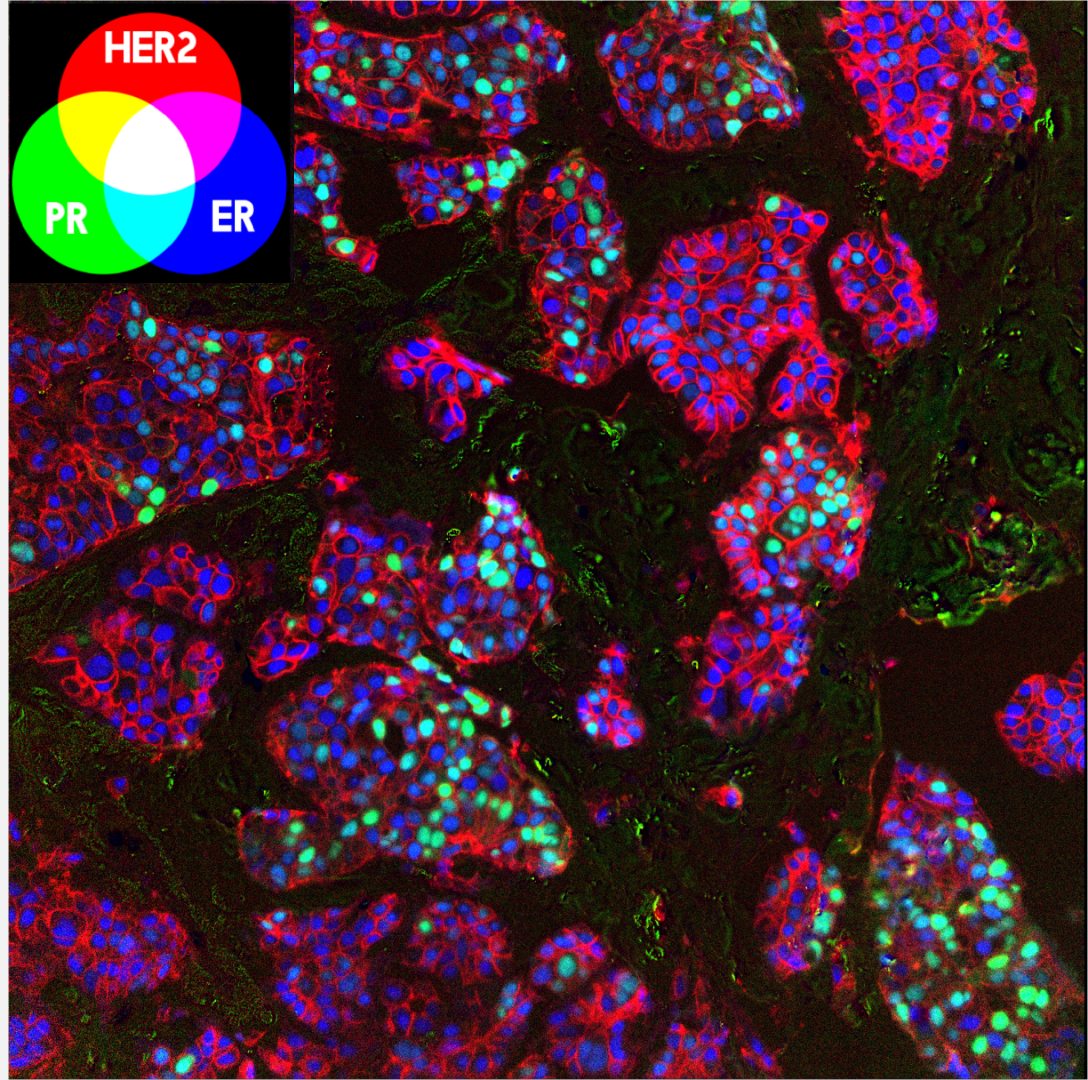
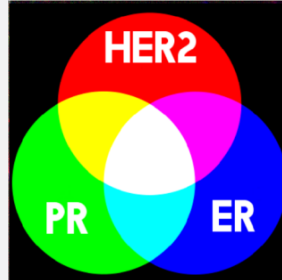
Multi to hyperplexed fluorescence imaging of whole section for higher spatial resolution and tissue context

Multiplexed IF

- 9 biomarkers (up to 60Ab)
- Multiple FISH

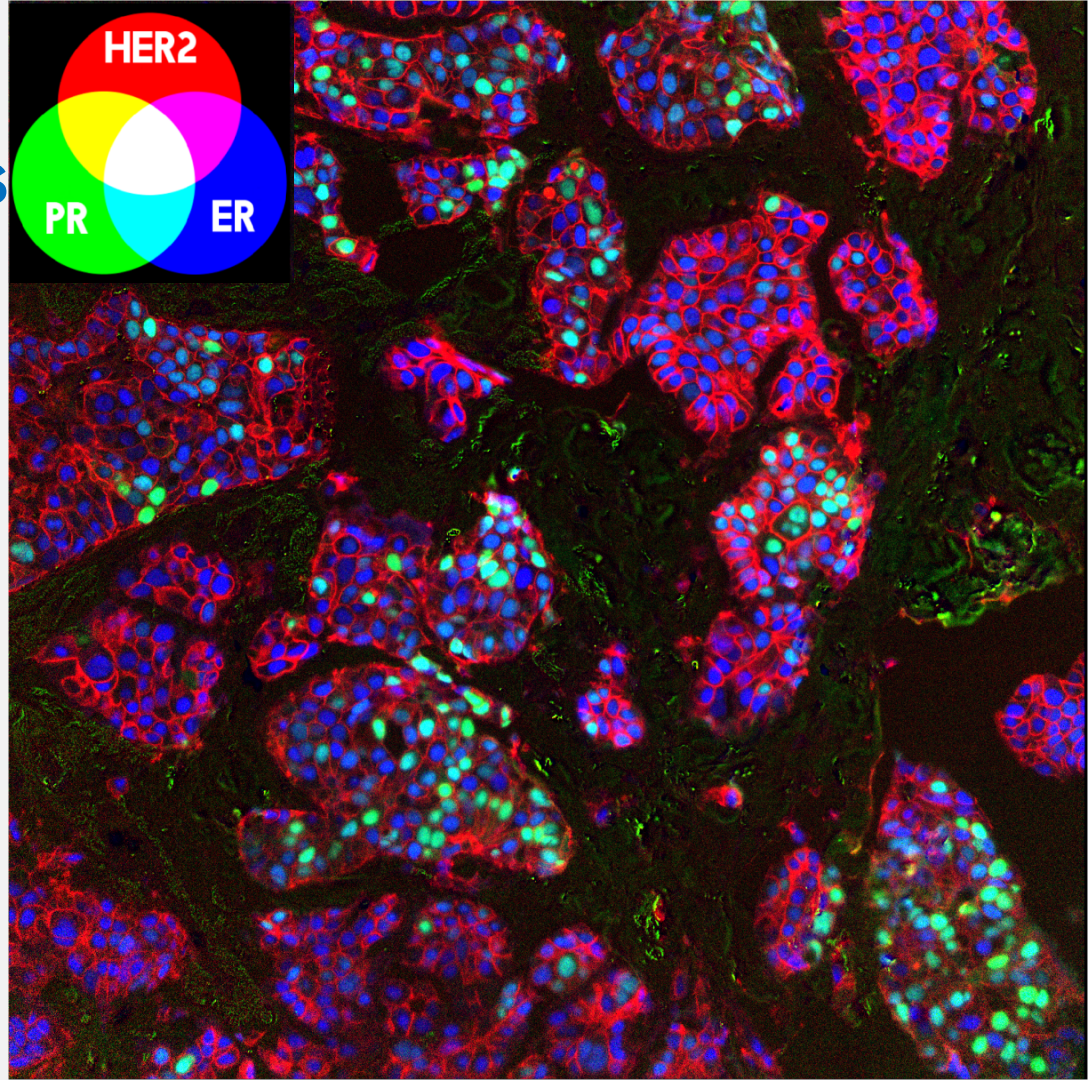
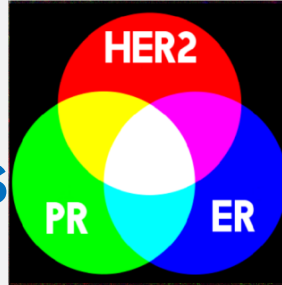


Gerdes et al. PNAS 2013;110:11982-11987



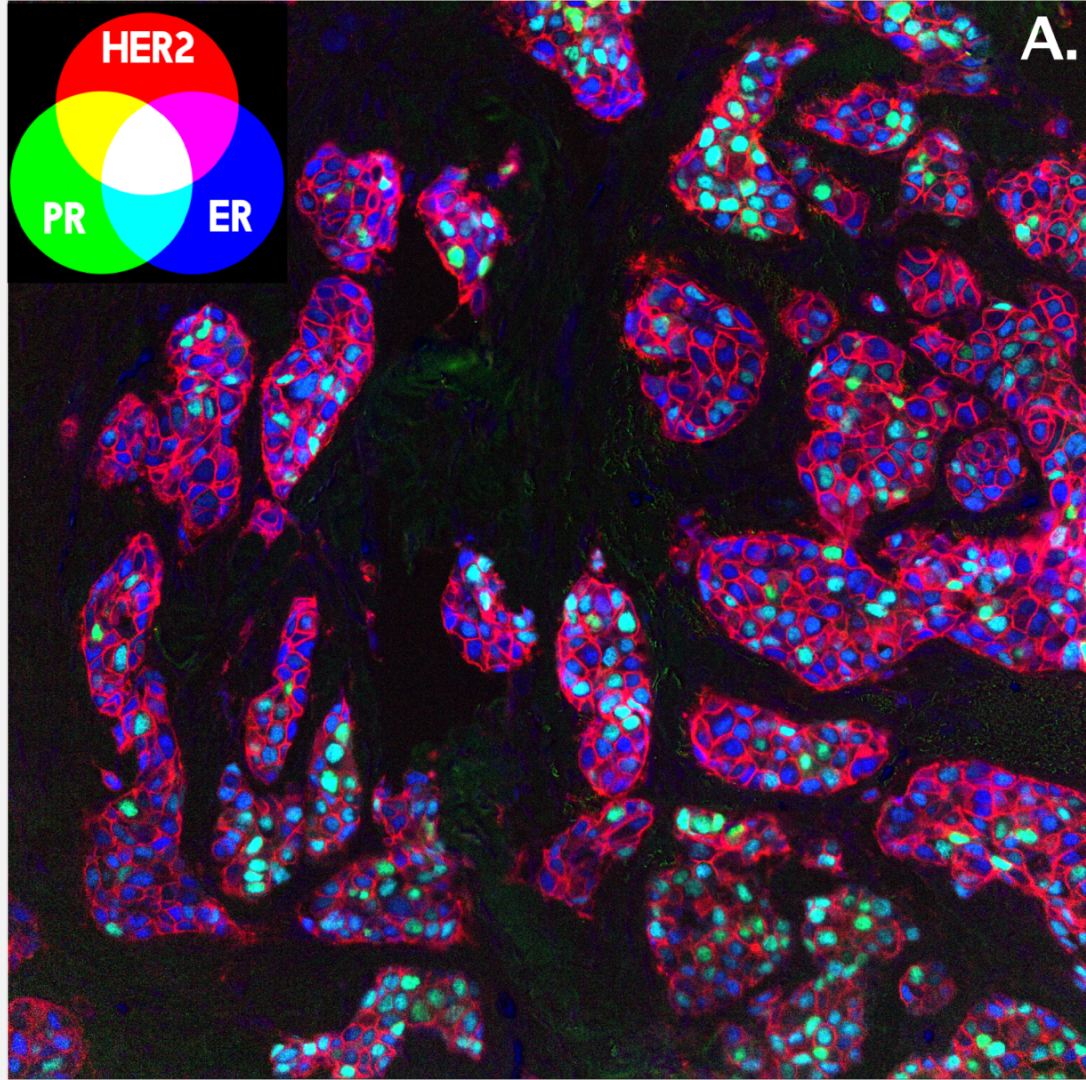
Heterogeneity Metrics

- Shannon Index
- Quadratic Entropy
- Pointwise Mutual Information
- Other indices



Data

- FFPE tissue 99 spot TMA
- 20x mag
- 4 Cancer types
 - ER(+) IDC (3 patients)
 - ER(+) ILC (5 patients)
 - ER(-) IDC (8 patients)
 - HER2(+) IDC (8 patients)
- 3 replicate cores/patient
- Fluorescent markers
 - Diagnostic markers
 - ER, HER2, PR
 - Structural markers
 - DAPI, Na⁺K⁺ATPase, S6, panCK
- 27 spots BC cell lines



Data

Spot #	Patient ID	# Cells
000	AL13-1	23 (1181)
031	AL13-1	222 (382)
026	AL13-2	72 (376)
055	AL13-2	604 (641)
060	AL13-2	420 (624)
005	AL13-3	433 (589)
046	AL13-3	327 (1629)
086	AL13-3	164 (600)

(a) ER(+) IDC

Spot #	Patient ID	# Cells
001	AL13-4	721 (249)
043	AL13-4	882 (192)
066	AL13-4	1065 (112)
011	AL13-5	2589 (166)
061	AL13-5	3339 (26)
080	AL13-5	2975 (52)
006	AL13-6	297 (621)
025	AL13-6	269 (458)
076	AL13-6	348 (246)
045	AL13-7	260 (192)
030	AL13-8	20 (125)
056	AL13-8	1062 (165)
096	AL13-8	479 (182)

(b) ER(+) ILC

Spot #	Patient ID	# Cells
002	AL13-9	0 (1032)
039	AL13-9	43 (779)
079	AL13-9	1 (1084)
012	AL13-10	0 (1173)
052	AL13-10	0 (185)
091*	AL13-10	0 (1779)
024	AL13-11	0 (849)
049	AL13-11	28 (831)
089*	AL13-11	0 (895)
007	AL13-12	3 (381)
034	AL13-12	1 (482)
062	AL13-12	52 (917)
017	AL13-13	17 (84)
036	AL13-13	4 (1055)
072	AL13-13	44 (1219)
020	AL13-14	1 (1322)
044	AL13-14	0 (2296)
071	AL13-14	8 (1414)
032	AL13-15	12 (764)
057	AL13-15	65 (532)
029	AL13-16	118 (876)
067	AL13-16	4 (804)
095	AL13-16	4 (1771)

(c) ER(-) IDC

Spot #	Patient ID	# Cells
003	AL13-17	147 (53)
038	AL13-17	209 (36)
068	AL13-17	276 (39)
015	AL13-18	69 (39)
041	AL13-18	771 (184)
078	AL13-18	319 (678)
013	AL13-19	245 (215)
053	AL13-19	824 (123)
090	AL13-19	970 (178)
023	AL13-20	1044 (757)
063	AL13-20	799 (229)
088	AL13-20	669 (101)
008	AL13-21	39 (162)
033	AL13-21	194 (44)
065	AL13-21	97 (7)
018	AL13-22	677 (6)
048	AL13-22	890 (2)
073	AL13-22	521 (5)
021	AL13-23	86 (57)
058	AL13-23	439 (8)
083	AL13-23	1048 (28)
028	AL13-24	126 (1724)
070	AL13-24	64 (1440)
093	AL13-24	309 (2079)

(d) HER2(+) IDC

a

1



2



3



4



5



6



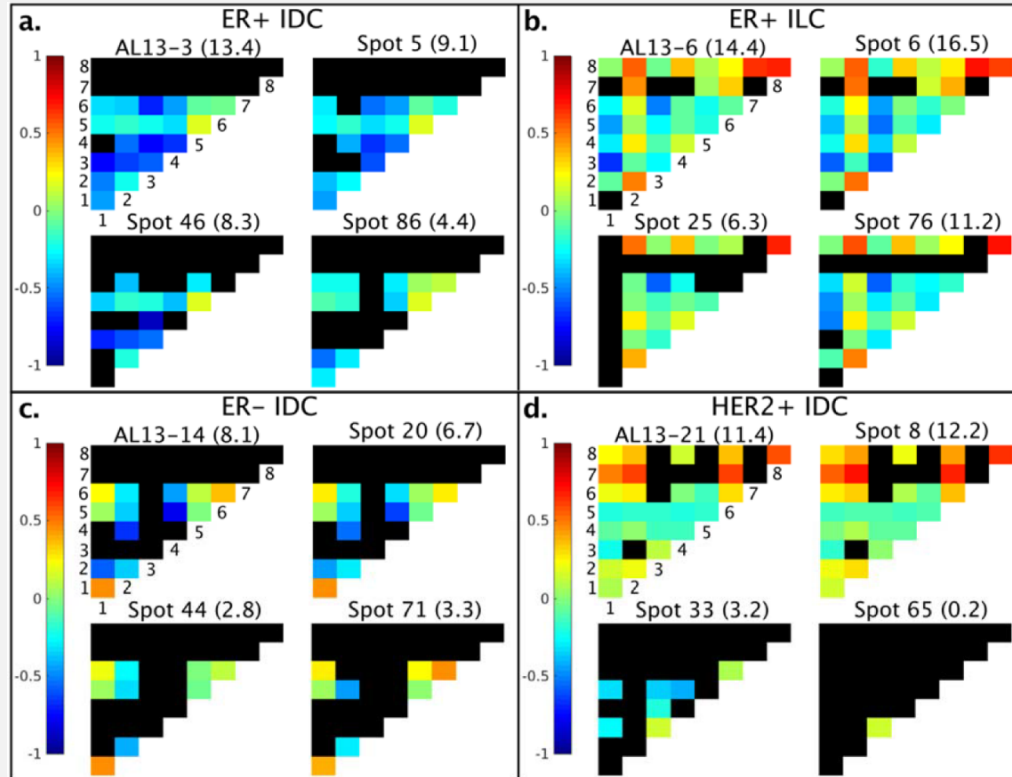
7



8



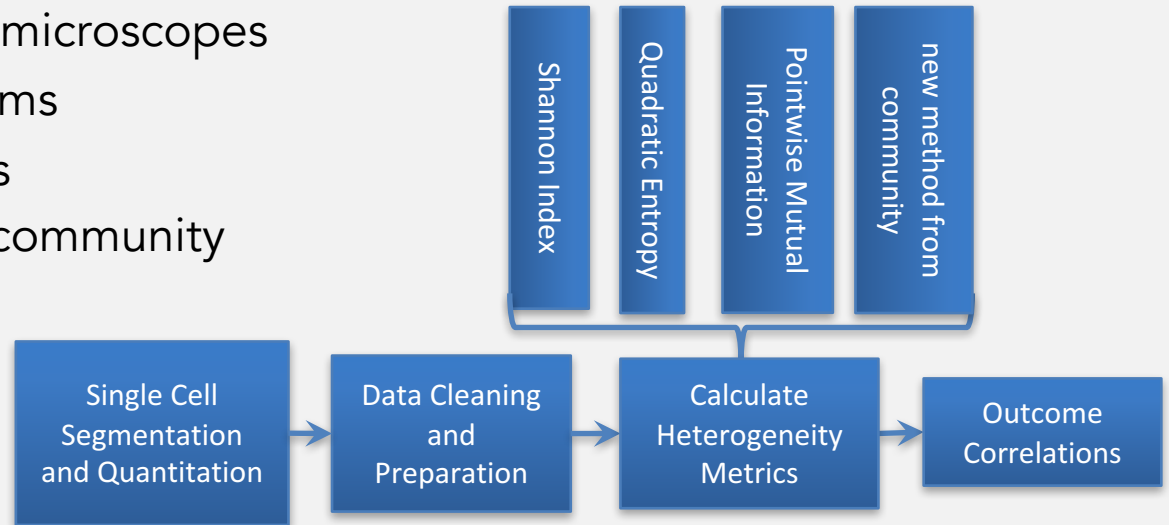
PMI maps as potential diagnostic biomarkers



Spagnolo, DM, et al. Journal of Pathology Informatics, 2016; 7:47

THRIVE: Tumor Heterogeneity Research Interactive Visualization Environment

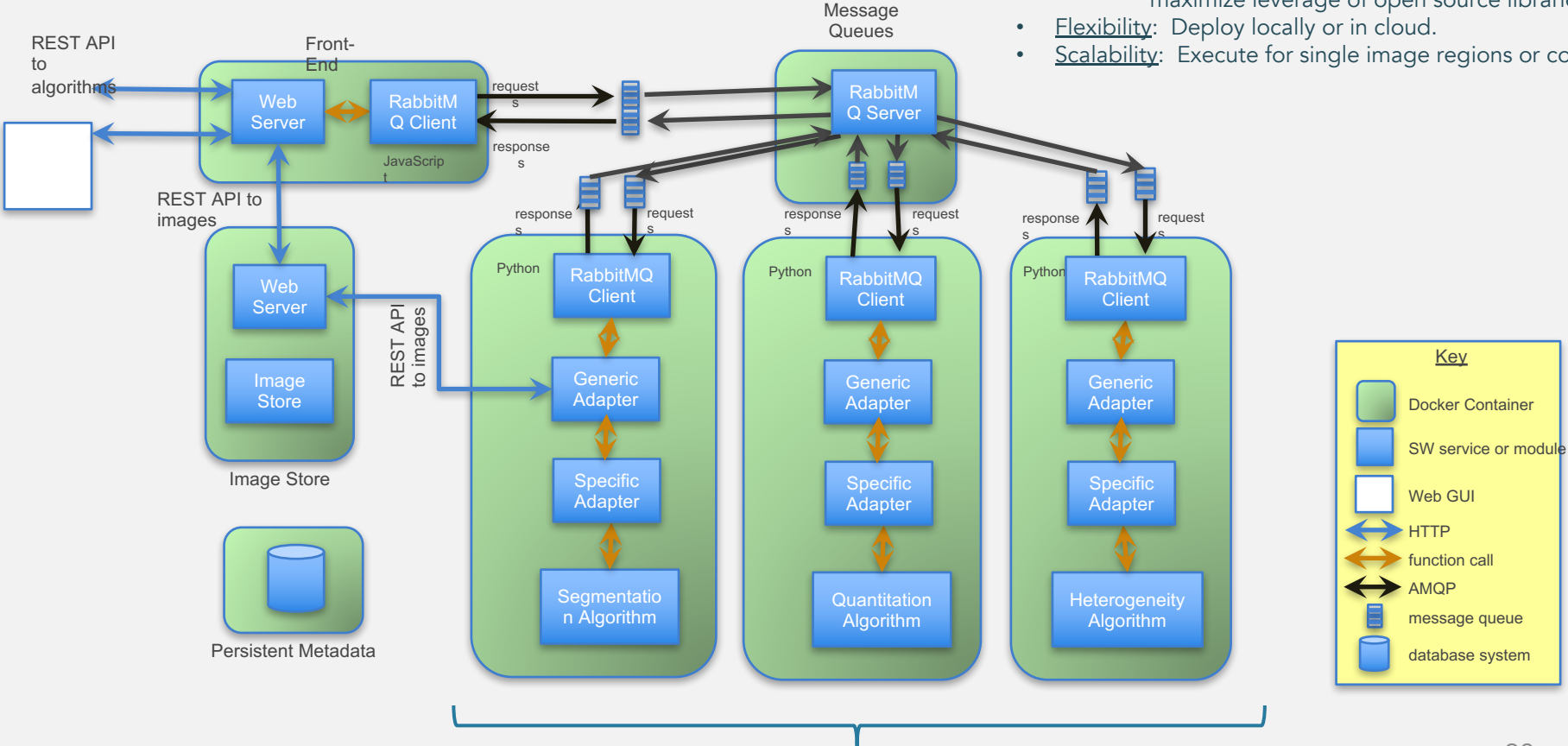
- Open software framework
- Compatible with standard microscopes
- Easy to contribute algorithms
- Easy to contribute datasets
- Actively used by research community



Software Architecture

Architectural drivers:

- Extensibility: Minimal effort to add more algorithms.
- Maintainability: Minimize application code, maximize leverage of open source libraries.
- Flexibility: Deploy locally or in cloud.
- Scalability: Execute for single image regions or cohort.



Key

- Docker Container
- SW service or module
- Web GUI
- HTTP
- function call
- AMQP
- message queue
- database system

Video Demonstration

(Click to run video.)

13TH for Tumor Heterogeneity

localhost/13th.html

Interactive Image Informatics Toolbox for Tumor Heterogeneity

Slides
AGA_200_3

Regions
012

Channels
DAPI

Segmentation Algorithms
WaveletNuclearSegmentation-v1.0.0

Quantitation Algorithms
CellQuantification-v1.0.0

Heterogeneity Algorithms
HeterogeneityMetrics-v1.0.0

HeterogeneityMetrics

Algorithm Parameters

Param	Value
Analysis Container	demoAnalysis
Feature Index	19
Region	012
Slide Name	AGA_200_3

Execute

WWWC
Pan
Zoom
Rectangle ROI

(678, 1153) to (1108, 1502)
There are 109 selected cells.
CD3: 368
CD20: 2048
CD45: 105
Diversity: 0.1244

AGA_200_3 Image #11
X=26, Y=142
Zoom:0.25
WWWC#3417/21616

Marker Expression within ROI

Box plot showing marker expression levels for CD3, CD4, CD20, and CD45. The y-axis ranges from 0 to 8000. CD20 shows the highest median expression, followed by CD3, CD4, and CD45.

Diversity within ROI

Histogram showing the distribution of diversity values within the ROI. The x-axis ranges from 0.05 to 0.3. The distribution is unimodal and centered around 0.1.

Execution List

Algorithm	Start Time	Status
HeterogeneityMetrics-v1.0.0	06:23:17 13:16:27	EXECUTION_FINISHED_SUCCESS

Median	E Col Max	Diversity	R	G	B
426.0	0.518878	0.000000	0.000000	0.000000	0.000000
3081.0	0.175801	0.000000	0.000000	0.000000	0.000000
112.0	0.124200	0.000000	0.000000	0.000000	0.000000
1726.0	0.515584	0.000000	0.000000	0.000000	0.000000
1441.0	0.502810	0.000000	0.000000	0.000000	0.000000

Timeline

- Summer 2017 – Version 0.1 available for demonstration, both as source code and cloud-hosted demonstration. Initial evaluators identified. Feedback solicited.
- Fall 2017 – Version 0.2 includes ability to upload and import lab-generated image sets. Additional feedback solicited.
- 2018 – Several iterative releases ramping up user base and having prioritized improvements identified by pilot users.
- April 2019 – Version 1.0 available.

Publications

1. Spagnolo DM, Gyanchandai R, Al-Kofahi Y, Stern AM, Gough A, Meyer DE, Ginty F, Sarachan B, Fine J, Lee AV, **Taylor DL, Chennubhotla SC.** (2016). *Pointwise mutual information quantifies intra-tumor heterogeneity in tissue sections labeled with multiple fluorescent biomarkers.* J. Pathol. Inform. 7(1): 47, doi: 10.4103/2153-3539.194839
1. Gough A, Stern AM, Maier J, Lezon T, Shun TY, Chennubhotla C, Schurdak ME, Haney SA, Taylor DL (2017) *Biologically Relevant Heterogeneity: Metrics and Practical Insights.* SLAS Discov. Mar;22(3):213-237. doi: 10.1177/2472555216682725. Epub 2017 Jan 6.
1. Nguyen, L., Tosun, B., Fine, J., Lee, A., **Taylor, L., Chennubhotla, C.** (2017) *Spatial statistics for segmenting histological structures in H&E stained tissue images,* IEEE Trans Med Imaging. 2017 Mar 16. doi: 10.1109/TMI.2017.2681519.
1. Nguyen, L., Tosun, B., Fine, J., **Taylor, L., Chennubhotla, C.** (2017) *Architectural patterns for differential diagnosis of proliferative breast lesions from histopathological images,* IEEE International Symposium on Biomedical Imaging (ISBI) Melbourne, Australia April, 2017
1. Tosun, B., Nguyen, L., Ong, N., Navolotskaia, O., Carter, G., Fine, J., **Taylor, L., Chennubhotla, C.** (2017) *Histological detection of high-risk benign breast lesions from whole slide images,* 20th International Conference on Medical Image Computing and Computer Assisted Intervention (MICCAI), Quebec City, Quebec, Canada 2017.
1. Jones, T., Nguyen, L., Tosun, B., **Chennubhotla, C.,** Jeffrey L Fine. (2017) *Computational Pathology versus Manual Microscopy: Comparison Based on Workflow Simulations of Breast Core Biopsies,* 106th Annual Meeting of USACP, San Antonio, Texas, March 2017

Acknowledgments

Chakra Lab

Lương Nguyễn

Dan Spagnolo

Maurice Marx

Dr. Burak Tosun

Dr. Shikhar Uttam

Dr. Filippo Pullara

Drug Discovery Institute

Dr. Lans Taylor

Dr. Bert Gough

Dr. Tim Lezon

Dr. Andy Stern

Dept. of Pathology

Dr. Jeffrey Fine

Magee-Womens RI

Dr. Rekha Gyanchandani

Dr. Adrian Lee

UPCI

Dr. Lin Zhang

GE Global Research

Yousef Al-Kofahi, PhD

Fiona Ginty, PhD

Jim Miller, PhD

Bo Wang, PhD

Alex Wei (intern)

Peihong Zhu

GE Healthcare

Andre Sublett

NIH-NCI

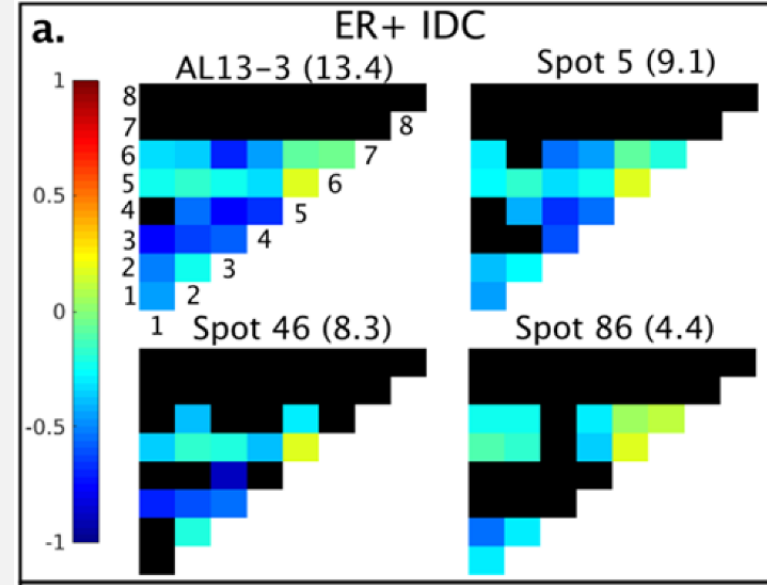
U01CA204826

NHGRI

BD2K U54HG008540 (Lung DBP)

PMI maps as potential diagnostic biomarkers

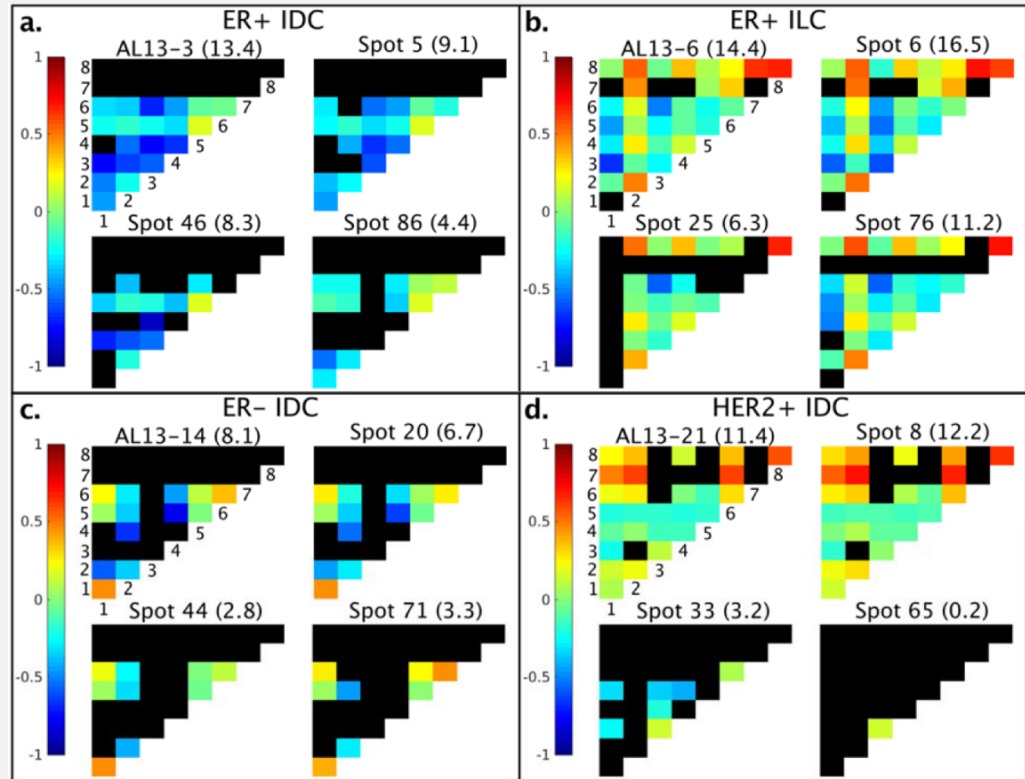
- PMI maps constructed for individual cores using the background distributions of cell phenotypes in the entire dataset, and pooled together for patient-level PMI (entire tumor) to better assess intratumor heterogeneity.
- Heterogeneity score assigned to each core/patient based on the entries in each PMI map



Spagnolo, DM, et al. Journal of Pathology Informatics, 2016; 7:47

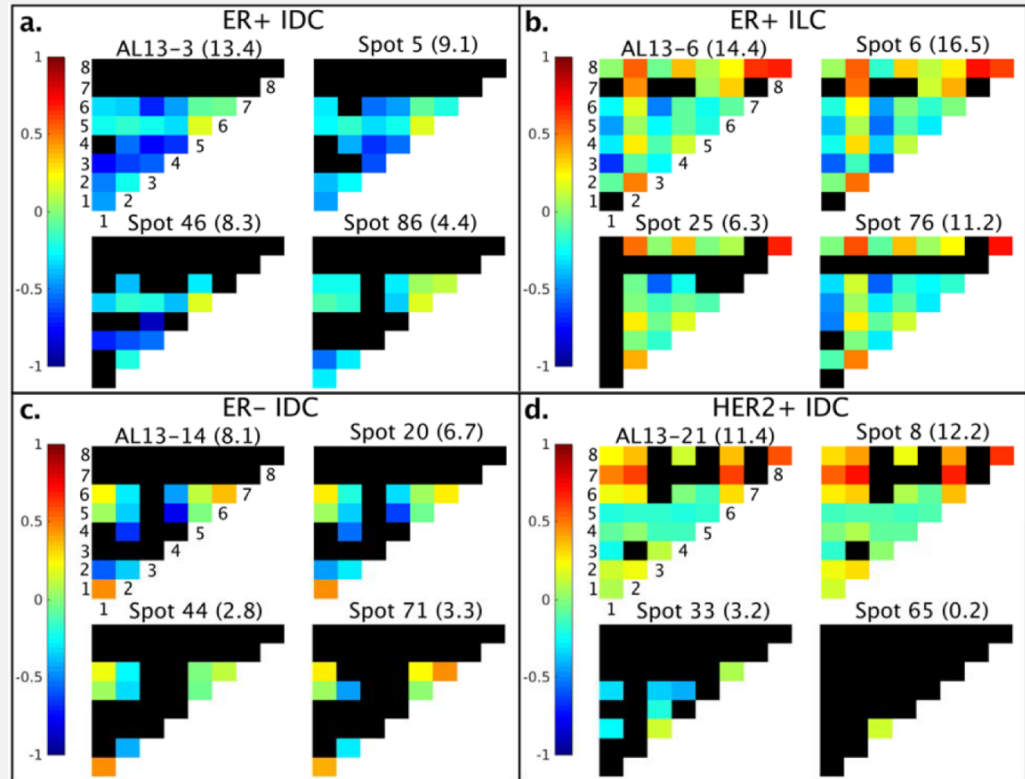
PMI Maps Exhibit Patterns that are Characteristic of Individual Patient Tumors

Heterogeneity score:
AL13-3 ER(+) IDC & AL13-6
ER(+) ILC show more
heterogeneity (difference
from background) than
AL13-14 ER(-) IDC & AL13-
21 HER2(+) IDC.



PMI Maps Exhibit Patterns that are Characteristic of Individual Patient Tumors

- core-level PMI maps for AL13-14 ER(-) IDC very similar => each core is a reasonable approximation for the patient-level analysis
- AL13-21 Her2(+) IDC has highly differing core-level PMI maps => high degree of intratumor heterogeneity in this patient.



PMI Maps Exhibit Patterns that are Characteristic of Individual Patient Tumors

- heterogeneity score (1-d) : simple low-level understanding of heterogeneity between or within patient samples
- PMI maps (2-d) provide a higher-level understanding, providing insights into the spatial relationships of different cell types which brings about the heterogeneity

